Received: December 28, 2023. Revised: January 19, 2024.

International Journal of
Intelligent Engineering & Systems

http://www.inass.org/

Improved Skill Optimization Algorithm Based Optimal Power Flow Considering Open-Access Trading of Wind Farms and Electric Vehicle Fleets

M. V. Ramesh[1] **K. Swarnasri[2]** **P. Muthukumar[1]** **Ponnam Venkata Kishore Babu[2]***

[1]*Department of Electrical and Electronics Engineering, Prasad V. Potluri Siddhartha Institute of Technology, Vijayawada - 520007, Andhra Pradesh, India*
[2]*Department of Electrical and Electronics Engineering, RVR & JC College of Engineering, Guntur - 522019, Andhra Pradesh, India*
* Corresponding author's Email: kishore.ponnam@gmail.com

Abstract: The paradigm shift towards sustainable energy sources has propelled research into enhancing the efficiency and reliability of power systems. This study introduces an advanced methodology for optimal power flow (OPF) by integrating the skill optimization algorithm (SOA) with considerations for open-access trading of wind farms and the integration of electric vehicle (EV) fleets. In order to improve exploration features of SOA, opposition-based learning (OBL) is used for diversifying the population. The proposed ISOA-based OPF model addresses the optimization of power flow in a multi-objective framework, aiming to minimize generation cost and minimize transmission loss while accommodating the open access trading between wind farms and EV fleet demands. The incorporation of open-access trading enables the effective utilization of surplus wind energy among interconnected power systems, fostering grid resilience and sustainable benefits. Simulation results on standard IEEE 30-bus and 57-bus test systems validate the efficacy of the proposed approach, showcasing improved system performance, reduced cost and power losses, and enhanced utilization of renewable resources in modern power grids. In the IEEE 30-bus, fuel costs are \$803.13/hr standard and \$935.2408/hr with extra trading. In the IEEE 57-bus, costs are \$37589.34/hr standard and \$37628.8/hr with additional trading. These results align with benchmarks, showcasing the method's efficacy in intricate problem-solving.

Keywords: Optimal power flow, Electric vehicle fleets, Open access trading, Wind farms, Skill optimization algorithm, Opposition-based learning.

1. Introduction

In the modern power system operation and control, the imperatives of sustainability, efficiency, and reliability have prompted a fundamental re-evaluation of traditional approaches. Optimal power flow (OPF) is one such approach optimizes power generation and distribution, vital in maintaining grid stability, minimizing losses, and maximizing efficiency. It balances generation and demand, ensuring cost-effectiveness, voltage stability, and proper utilization of resources in modern power systems [1]. Conventional optimization approaches for solving optimal power flow (OPF) problems face challenges due to the non-linearity, high dimensionality, and combinatorial complexity inherent in power systems. These methods struggle to handle the vast solution space, constraints, and discrete variables involved. Meta-heuristics, notably algorithms like genetic algorithms, particle swarm optimization, and evolutionary computation, play a pivotal role due to their ability to efficiently navigate complex, non-linear spaces, offering robust, near-optimal solutions for OPF [2]. Their adaptability, ability to handle multi-objective optimization, and capacity to overcome local optima make meta-heuristics indispensable in addressing the intricate nature of modern power system optimization within manageable computational resources.

To address the OPF issue in large-scale systems, a novel variable neighbourhood descent metaheuristic method is put forth in [3]. It blends a metaheuristic approach with a mixed-integer nonlinear programming paradigm. An efficient whale optimization algorithm (EWOA) is put out in [4] to address OPF issues. By integrating two novel movement strategies—whale surrounding prey using levy motion for better exploration and seeking for prey using brownian motion that balances exploration and exploitation—the EWOA-OPF improves upon the conventional WOA. A new approach to multi-objective OPF problem solving is presented in [5], and it is based on the recently created slime mold algorithm (SMA). The method is subjected to non-dominated Pareto sorting and crowding techniques in order to preserve a collection of varied trade-off solutions. By fusing differential evolution (DE) with self-adaptive particle swarm optimization (PSO), a unique fuzzy adaptive hybrid method is created in [6]. It effectively resolves three test systems' worth of multi-objective OPF issues, reducing costs, losses, and emissions while taking into account realistic restrictions. Three Rao algorithms are shown in [7] to handle OPF issues in three typical test systems while taking into account technical and economical goal functions. The voltage collapse proximity index (VCPI) is used in [8] as part of a multi-objective optimization strategy to enhance static voltage stability in normal, emergency, and stressful operation scenarios. The multi-case research findings are ranked using a preference selection index approach to determine the optimal operational solution. An improved salp swarm method (ISSA) is suggested in [9] to balance the exploration-exploitation trade-off and avoid local optima while solving non-smooth OPF problems. It improves both the exploration and exploitation of the basic SSA by merging random mutation and adaptive exploitation. The marine predator algorithm (MPA) is presented in [10] as a solution to a number of different single-objective OPF issues. The algorithm is able to identify optimum solutions through both exploratory and exploitative search, thanks to its unique foraging style and the biological interplay between predators and prey. Arithmetic optimization algorithm (AOA) and sequential approximation (SA) are used in [11] to address the OPF issue in direct current (DC) networks using a hybrid master-slave approach. A hybridization of the backtracking search algorithm (BSA) and grey wolf optimization (GWO) is proposed in [12] to solve the OPF issue and incorporate the unified power flow controller (UPFC). The OPF problem is solved in [13] by developing whale and moth-flame optimization (WMFO), which addresses problems including local optima entrapment, premature convergence, and stagnation. The use of gorillas' group behaviours in the created gorilla troops optimization (GTO) in [14] to solve the multi-objective OPF in electrical power systems is what makes it innovative. Its capacity to balance system limits with the optimization of fuel prices, power losses, and hazardous emissions is its main contribution. The neighbourhood dimension learning (NDL) search method is used in [15] to present an upgraded slime mould algorithm (ESMA) that improves the speed and accuracy of optimization for solving the OPF issue. In [16], the quick non-dominated sorting, crowding distance, and archive selection techniques are combined in an efficient manner using the multi-objective search group algorithm (MOSGA), which results in the acquisition of a non-dominated set in a single run. An improved equilibrium optimizer (EEO) algorithm is developed in [17] to solve optimal power flow (OPF) problems more quickly and effectively than previous algorithms. This algorithm incorporates a new performance reinforcement strategy with the Lévy flight mechanism.

Even though these methods worked successfully to address OPF in traditional power systems, OPF in contemporary power systems has to be reframed. The incorporation of sustainable energy sources, namely wind farms, in conjunction with the rise of electric vehicle (EV) fleets has presented hitherto unseen challenges and prospects for optimizing power systems. Algorithms for OPF have proven essential in coordinating power system activities, with the goals of reducing losses, improving grid resilience, and meeting changing customer needs.

In [18], marine predators algorithm (MPA) is introduced to solve the multi-regional OPF problem, considering load and generation variability. In [19], a modified Rao algorithm (MRao-2) is proposed for OPF incorporating renewable energy sources. It demonstrates the effectiveness of MRao-2 on standard test systems and compares it to other algorithms, showing superior performance in solving the OPF problem. In [20], an OPF solution is presented based on jellyfish search optimization considering the uncertainty of RESs. In [21], a bio-inspired heuristic algorithm is proposed for solving the OPF problem in hybrid power systems. In [22], an OPF solution with stochastic wind power is analysed using the Lévy coyote optimization algorithm (LCOA). In [23], OPF is addressed by incorporating stochastic wind and solar generation using metaheuristic optimizers. In [24], a novel metaheuristic method is introduced for the optimal power flow solution of wind-integrated power systems. In [25], the white sharks algorithm (WSA) is introduced for solving the OPF in power systems with renewable energy sources. In [26], an evolutionary-based multi-objective OPF is addressed considering real-time uncertainties in wind farms and load demand. In [27], fire hawk optimizer (FHO) is utilized for solving the probabilistic OPF problem with RESs in distribution networks. In [28], a gradient bald eagle search optimization algorithm (GESA) is developed with a local escaping operator to integrate renewable energy and vehicle-to-grid uncertainty into OPF. In [29], a hybrid AEO-CGO approach is developed for OPF analysis with RESs uncertainty. In [30], an adaptive geometry estimation-based multi-objective differential evolution (DE) is introduced for multi-objective OPF in thermal-wind-solar power systems. In [31], a modified artificial hummingbird algorithm (MHBA) is applied for OPF and generation capacity in power networks considering RESs. In [32], OPF is presented to power systems with wind energy using a highly effective metaheuristic algorithm. In [33], leader supply-demand-based optimization (LSDO) approach is proposed for the large-scale optimal power flow problem considering renewable energy generations.

These studies demonstrate the usefulness of metaheuristics in solving the OPF problem in both modern power systems with RESs and EVs and conventional power systems. The majority of metaheuristics, however, have issues with local traps and inadequate exploration/exploitation search characteristics. As a result, researchers are motivated to provide novel algorithms and enhance current ones in accordance with the no free lunch (NFL) theorem [34]. As a result, this work presents a novel method for tackling the complexities of contemporary power networks by combining the skill optimization algorithm (SOA) [35] and opposition-based learning with open-access wind farm trade and EV fleet integration within the OPF framework.

The integration of open-access trade facilitates the effective distribution of excess electricity from wind farms among linked grids, promoting cooperation and adaptability to fluctuating renewable energy outputs. Furthermore, depending on how well management tactics work, the integration of EV fleets creates a dynamic demand that may either strain or augment the grid. When properly implemented within the OPF framework, this integration may both reduce the risk of grid instability and maximize the ability of EVs to function as distributed energy resources, which will increase the stability and flexibility of the grid.

The following are the major contribution of this paper with respect to literature works.

1. Innovative IFOA-based OPF model: The research introduces a cutting-edge IFOA-based OPF model specifically crafted to optimize power flow. This model uniquely considers the intricate interplay between integrating EV fleets and the trade dynamics of wind farms.

2. Enhanced system performance: Through comprehensive simulations on industry-standard test systems, the proposed methodology demonstrates its effectiveness and superiority. It showcases the potential to significantly enhance system performance by maximizing power flow efficiency.

3. Reduced power losses: The novel model aims to mitigate power losses within power grids. By doing so, it offers a promising solution to curtail unnecessary wastage and enhance overall grid efficiency.

4. Facilitates seamless integration of EVs and renewable energy: A key highlight lies in the model's ability to facilitate the smooth integration of electric vehicles and renewable energy sources into modern power grids. This feature holds immense promise for advancing sustainable energy initiatives.

The subsequent sections of the paper are structured as follows: Section 2 delineates the mathematical models applied to wind farms, EV fleets, and open access trading. Section 3 delves into the optimization problem, addressing both equal and unequal constraints. Section 4 elucidates the fundamental SOA alongside its enhanced iteration. Following this, section 5 presents the results obtained, culminating in section 6, which comprehensively underscores the primary discoveries of this study.

2. Modelling of theoretical concepts

This section provides the concepts of wind farms (WFs), EV fleets and open access trading modelling comprehensively.

2.1 Wind farms

Wind farms (WFs) harness wind energy to generate electricity, comprising multiple turbines strategically positioned to optimize power generation. They contribute significantly to renewable energy goals, offering a clean, sustainable power source while facing challenges related to variable output and efficient integration into power grids.

By regulating WF converter voltage magnitude $|V_{wt}|$ and its phase angle δ_{wt} with respect to grid-

Received: December 28, 2023. Revised: January 19, 2024.

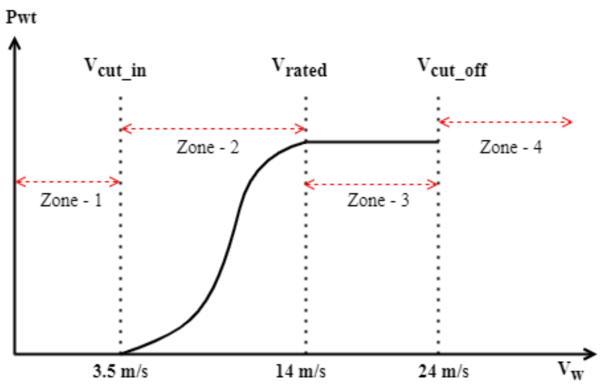

Figure. 1 Typical WT generation (watts) with steady wind speed (in meters/sec)

voltage magnitude $|V_g|$ and load angle δ_g, the exchange of active and reactive power flows through transformer can be controlled effectively. Since, it can able to adjust bus voltage magnitude and active power, the WT integrated bus can be modelled as generator bus in load flow studies. Mathematically,

$$P_{wt} = \begin{cases} 0 & Zone - 1 \\ P_{wt,r}(0.5\rho A_s V_{wt}^3) & Zone - 2 \\ P_{wt,r} & Zone - 3 \\ 0 & Zone - 4 \end{cases} \quad (1)$$

$$Q_{wt} = P_{wt} \times tan(\theta_{wt}) \quad (2)$$

$$\begin{matrix} Zone - 1 & V_{wt} < V_{cun\_in} \\ Zone - 2 & V_{cun\_in} < V_{wt} < V_{wt,r} \\ Zone - 3 & V_{wt,r} < V_{wt} < V_{cun\_off} \\ Zone - 4 & V_{wt} > V_{cun\_off} \end{matrix} \quad (3)$$

where P_{wt} and Q_{wt} are the active and reactive powers of WT, respectively; θ_{wt} is the power factor (*pf*) angle of WT converter, $P_{wt,r}$ is the rated power of WT, ρ is the air density, A_s is the WT swept area, V_{wt} is the speed of wind at a specific time, $V_{wt,r}$ is the rated speed of WT, V_{cun_in} is the cut-in speed at which WT starts generation, V_{cun_off} is the cut-off speed at which WT stops generation due to high wind speed.

2.2 Electric vehicle fleets

Electric vehicle (EV) fleets consist of multiple electric cars or vehicles operated by organizations or communities. They offer sustainable mobility, reducing emissions and dependency on fossil fuels. Managing their charging patterns and integrating them smartly into grids pose challenges and opportunities for grid stability and energy management. The arrangement of EV fleet for grid-integration is given in Fig. 2.

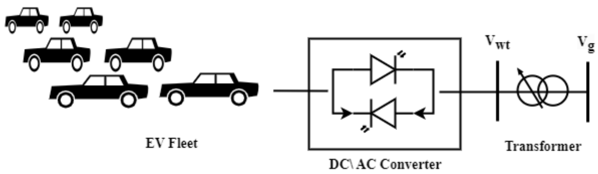

Figure. 2 Schematic diagram of EV fleet

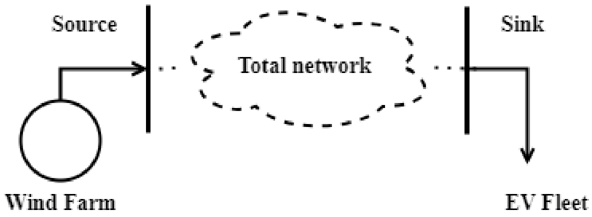

Figure. 3 Schematic representation of open access trading between wind farm and EV fleet

$$P_{ef} = N_{cp,s} \times N_{cp,p} \times P_{ev,r} \quad (4)$$

$$Q_{ef} = N_{cp,s} \times N_{cp,p} \times P_{ev,r} \times tan(\theta_{ef}) \quad (5)$$

where P_{ef} and Q_{ef} are the active and reactive power demands of EV fleet, respectively; θ_{ef} is the power factor (*pf*) angle of EV fleet converter, $N_{cp,s}$ and $N_{cp,p}$ are the number of charging ports arranged in series and parallel combinations, respectively.

2.3 Open access trading

Open-access trading facilitates the exchange of surplus energy among interconnected power systems or entities. It enables efficient utilization of excess renewable energy, like wind or solar power, optimizing resources and fostering collaboration between grids, promoting reliability, and balancing varying energy demands.

Bilateral open access market trading terms stipulate that source bus (wind farm) must supply the necessary quantity of load demand at sink bus (EV fleet) as shown in Fig. 3. The independent system operator (ISO) must enable the transmission system without sacrificing system security or congestion control in order to allow these transactions.

Under ideal circumstances, the mathematical power balance for each of these bilateral transactions in the network,

$$P_{wt} = -P_{ef} \quad (6)$$

Moreover, wind farms may store their excess power produced in energy storage systems or inject it into the main grid.

3. Problem formulation

The major objective of the OPF problem is to minimize fuel costs for power generation. The objective function is seen as a quadratic function of the active power output of the generating units and represents the system's total generation cost and is given by,

$$P_{cost} = \sum_{k=1}^{NG}\{a_k P_{g,k}^2 + b_k P_{g,k} + c_k\} \tag{7}$$

The following are the major equal and unequal operational constraints for handing OPF problem.

$$|V_k|_{min} \le |V_k| \le |V_k|_{max} \qquad \forall k = 1{:}\,nbus \tag{8}$$

$$a_{k,min} \le a_k \le a_{k,max} \qquad \forall k = 1{:}\,ntap \tag{9}$$

$$|I_k| \le |I_k|_{max} \qquad \forall k = 1{:}\,nline \tag{10}$$

$$P_{g,k,min} \le P_{g,k} \le P_{g,k,max} \qquad \forall k = 1{:}\,NG \tag{11}$$

$$Q_{g,k,min} \le Q_{g,k} \le Q_{g,k,max} \qquad \forall k = 1{:}\,nsh \tag{12}$$

$$Q_{sh,k,min} \le Q_{sh,k} \le Q_{sh,k,max} \qquad \forall k = 1{:}\,nsh \tag{13}$$

$$\left(\sum_{k=1}^{NG} P_{g,k} + \sum_{k=1}^{NWT} P_{wt,k}\right) = \left(\sum_{k=1}^{nbus} P_{d,k} + \sum_{k=1}^{NEV} P_{evf,k} + P_{loss}\right) \tag{14}$$

$$\left(\sum_{k=1}^{NG} Q_{g,k} + \sum_{k=1}^{NWT} Q_{wt,k}\right) = \left(\sum_{k=1}^{nbus} Q_{d,k} + \sum_{k=1}^{NEV} Q_{evf,k} + Q_{loss}\right) \tag{15}$$

where NG is the number of generators in the system, a_k , b_k and c_k are the cost coefficients of generator-k, respectively; $P_{g,k}$ is the output power from generator-k, P_{cost} is the total cost of real power generation, P_{loss} and Q_{loss} are the real and reactive power loss, respectively; $P_{d,k}$ and $Q_{d,k}$ are the real and reactive power demand of bus-k, respectively; NWT is the number of wind farms, $Q_{sh,k}$ is the shunt reactive power injection at bus-k, nsh is the number of shunt VAr control locations, $P_{g,k}$ and $Q_{g,k}$ are the real and reactive power generations by generator-k, respectively; $|I_k|$ is the current flow in line-k, $nline$ is the number of transmission lines, a_k is the tap-changer settings at bus-k, $ntap$ is the number tap-changers in the network, $|V_k|$ is the voltage magnitude of bus-k, $nbus$ is the number of buses in the system, min and max indicates the minimum and maximum limit of the variable, respectively.

4. Solution methodology

The solution methodology of OPF problem is developed based on recent metaheuristic skill optimization algorithm (SOA) with opposition-based learning (OLB). This section explains the basic mathematical model of SOA and improved SOA (ISOA) with OBL strategy.

4.1 Skill optimization algorithm

This section introduces the skill optimization algorithm (SOA), a population-based method driven by individuals aiming to improve skills. They serve as potential solutions to an optimization problem, their positions in the algorithm reflecting decision variables. Initially randomized, these positions form the SOA population, mathematically represented by matrix S given in Eq. (16). Here, S_i signifies each candidate solution, while $s_{i,d}$ denotes the value proposed by the *i*th member for the *d*th variable. N represents SOA members, and m, the variables. Placing members in problem variables allows objective function evaluation. Resulting values are mathematically depicted through a vector in Eq. (17). The vector F in Eq. (18) represents objective function values, with F_i denoting the value from the *i*th solution.

$$S = [S_1 \quad S_2 \quad \cdots \quad S_i \quad \cdots \quad S_N]_{N\times m}{}^T \tag{16}$$

$$S_i = [s_{i,1} \quad s_{i,2} \quad \cdots \quad s_{i,d} \quad \cdots \quad S_{N,i}]_{1\times m}{}^T \tag{17}$$

$$F = [F_1(S_1) \quad \cdots \quad F_i(S_i) \quad \cdots \quad F_N(S_N)]_{1\times m}{}^T \tag{18}$$

The best and worst values pinpoint the corresponding members, regularly updated in each iteration alongside the population. SOA's member updates occur in exploration and exploitation phases. Exploration mimics skill learning from experts, promoting diverse movements. Exploitation mirrors individual effort for skill enhancement, focusing on local improvements. SOA balances both phases for global and local searches. Exploration allows diverse movement patterns, expanding search scope, while exploitation concentrates on local searches for better solutions. This dual-phase design boosts SOA's ability to scan the space accurately and converge towards optimal solutions.

4.1.1. Skill acquisition from experts

In exploration phase, each SOA member learns from a community expert. Their quality aligns with their objective function value, wherein the expert is a member with superior conditions based on this value. All members with better objective function values constitute the 'experts set', from which a random expert trains each member. This expert isn't necessarily the best solution but guides diverse movements, enabling global search. New positions are accepted if they enhance the objective function value, modelled by Eqs. (19) and (20) in this update phase.

$$S_i^{P1}: s_{i,d}^{P1} = s_{i,d} + r \times \left(Ex_{i,d} - R \times s_{i,d}\right) \tag{19}$$

where $Ex_i = S_k$ and $F_k < F_i$ and k is randomly selected from $\{1,2,\dots,N\}, k \neq i$.

$$S_i = \begin{cases} S_i^{P1} & F_i^{P1} < F_i \\ S_i & else, \end{cases} \tag{20}$$

Here, S_i^{P1} stands for the recalculated status of the *i*th candidate solution derived from the initial phase, $s_{i,d}^{P1}$ refers to its dth dimension, while F_i^{P1} signifies its objective function value, Ex_i represents the expert selected to mentor and instruct the *i*th member of the population, with $Ex_{i,d}$ indicating its *d*th dimension, r denotes a random number within the range of 0 to 1, and R signifies a randomly chosen number from the set {1, 2}.

4.1.2. Skill improvement based on practice and individual effort

In exploitation phase, SOA focuses on individual skill enhancement post-learning. SOA simulates this as local search, intensifying exploitation. Members seek better conditions nearby to boost their objective function (skill level). Newly calculated positions are accepted if they improve the function, expressed through Eq. (21) and (22) in this update phase.

$$S_i^{P2}: s_{i,d}^{P2} = \begin{cases} s_{i,d} + \left(\frac{1-2r}{k}\right) s_{i,d} & r < 0.5 \\ s_{i,d} + \left(\frac{l_{b,j} - r(u_{b,j} - l_{b,j})}{k}\right) & else, \end{cases} \tag{21}$$

$$S_i = \begin{cases} S_i^{P2} & F_i^{P2} < F_i \\ S_i & else, \end{cases} \tag{22}$$

where S_i^{P2} represents the updated status of the *i*th candidate solution following the second phase, $s_{i,d}^{P2}$ denotes its *d*th dimension, while F_i^{P2} signifies its objective function value, k stands for the iteration counter, and $l_{b,j}$ and $u_{b,j}$ denote the lower and upper bounds, respectively, of the *j*th variable.

4.2 Improved skill optimization algorithm

The study bolsters SOA by preserving population diversity, promoting convergence toward the global optimum. The enhanced ISWO (ISWO) incorporates opposition-based learning (OBL), fostering solution diversity. OBL aids in exploring the search space effectively by computing solutions opposite to candidates, revealing promising areas for exploration.

$$\bar{S}_i = u_b + l_b - S_i \tag{23}$$

where $\bar{S}_i$ is a population initiated in the opposite direction.

5. Results and discussion

Simulations are performed on IEEE 30-bus and 57-bus test systems for base case and with open access trading in MATLAB R2023b environment.

5.1 IEEE 30-bus system

The test system has a total load of 283.40 MW and 126.20 MVAr, respectively. It has six generator buses i.e., buses 1, 2, 5, 8, 11, and 13. Among these, buses 11 and 13 are treated as wind farms and buses 10 and 24 are as EV fleets. The schematic diagram with these modifications is given in Fig. 4.

Case 1: The performance of the system is evaluated using NR load flow with generation schedule of standard test system data. The total operating cost for this case is 828.5192 \$/hr. Further, the losses are registered as 8.585 MW and 34.43 MVAr, respectively.

Case 2: The performance of the test system is re-evaluated using OPF with optimally determined schedule. The total operating cost for this case is 803.13 \$/hr. Further, the losses are registered as 9.679 MW and 39.24 MVAr, respectively.

Case 3: It is assumed that EV fleets at buses 10 and 24 are required to meet demand of 20 MW and 15 MW, respectively. By considering an operating power factor of 0.95 lagging, the reactive power demand is determined. The same amount of load demand is supposed to be supplied by wind farms at buses 11 and 13, respectively. The operating power factor of wind farms are treated as 0.867 leading. By these assumptions, the reactive power generation of wind farms are determined. For these open access trading, the operating cost is determined by satisfying all operating conditions. By EV fleets, the total load demand is raised to 318.4 MW and 137.7 MVAr, respectively. The total operating cost for this case is 935.2408 \$/hr. Further, the losses are

Received: December 28, 2023. Revised: January 19, 2024.

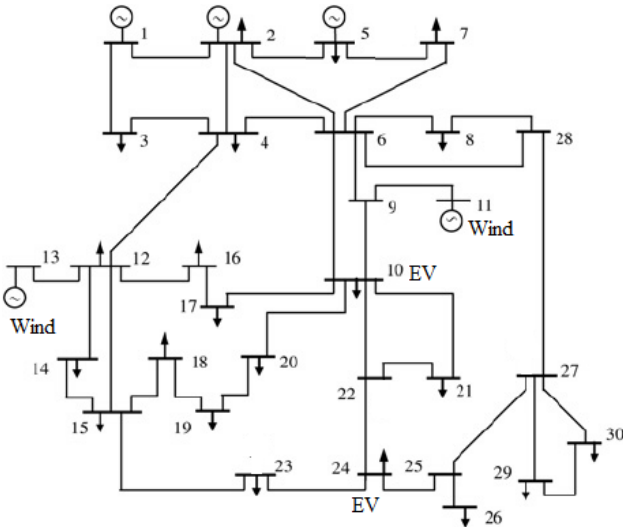

Figure. 4 Schematic diagram of modified IEEE 30-bus

registered as 11.552 MW and 51.03 MVAr, respectively.

5.2 IEEE 57-bus system

The test system has a total load of 1250.8 MW and 336.4 MVAr, respectively. It has six generator buses i.e., buses 1, 2, 3, 6, 8, 9, and 12. Among these, buses 2, 6 and 9 are treated as wind farms and buses 4, 11 and 21 are as EV fleets. The schematic diagram with these modifications is given in Fig. 5.

Case 1: The performance of the system is evaluated using NR load flow with generation schedule of standard test system data. The total operating cost for this case is 35296.34 $/hr. Further, the losses are registered as 8.585 MW and 34.43 MVAr, respectively.

Case 2: The performance of the test system is re-evaluated using OPF with optimally determined schedule. The total operating cost for this case is 37589.34 $/hr. Further, the losses are registered as 54.362 MW and 239.39 MVAr, respectively.

Case 3: It is assumed that EV fleets at buses 4, 11 and 21 are required to meet demand of 10 MW, 7.5 MW and 5 MW, respectively. The same amount of load demand is supposed to be supplied by wind farms at buses 2, 6 and 9, respectively. For these open access trading, the operating cost is determined by satisfying all operating conditions. By EV fleets, the total load demand is raised to 1273.3 MW and 343.8 MVAr, respectively. The total operating cost for this case is 37628.8 $/hr. Further, the losses are registered as 54.954 MW and 240.99 MVAr, respectively.

5.3 Comparative study

In literature, the simulations are done for

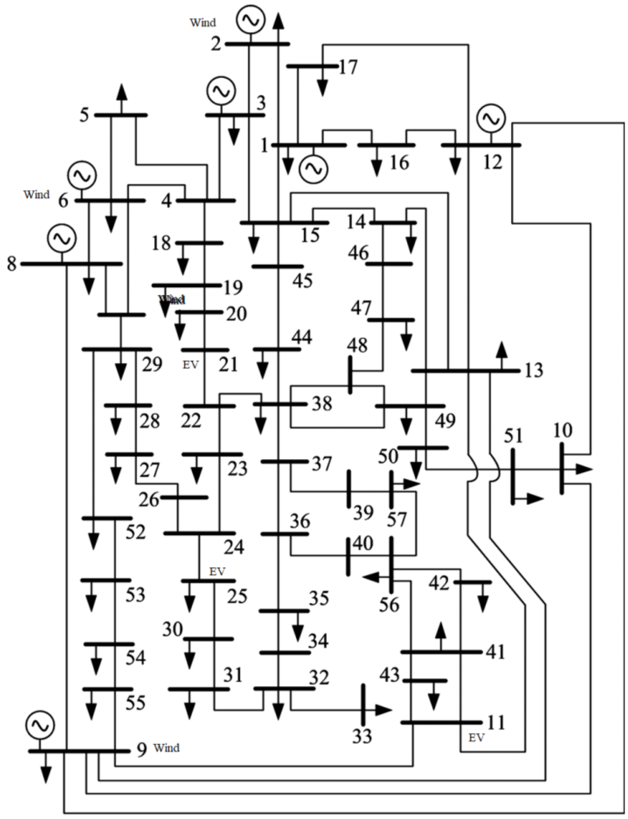

Figure. 5 Schematic diagram of modified IEEE 57-bus

different test systems for various scenarios/ single or multi-objective functions, this section is used for comparing only results on IEEE 30-bus and 57-bus for base case without considering any open access trading, i.e., Case 2 for both the systems in Table 1.

The results of 30-bus system are given in Table 2. It can be seen that the results of proposed method are better than MOPSO [8] and slightly poor than SMA [5], MOSGA [16], WMFO [13], EEO [17], ISSA [9], Rao-3 [7], FAHSPSO-DE [6], EWOA [4], GTOT [14], MPA [10], ESMA [15] and WO-BSA [12]. This is due to the fact that the slight difference in the data of cost coefficients, control variables and line flow limits. However, the standard data defined in [1] is used in this work and the results are well agreement with benchmarking results of [1].

The results of 57-bus system are given in Table 3. It can be seen that the results of proposed method are better than MOPSO [8], MOSGA [16], ISSA [9], Rao-3 [7], FAHSPSO-DE [6] and WMFO [13]. Further, the results obtained by proposed method are well competitive with the benchmarking results given by MATPOWER Software [1].

6. Conclusion

Efforts towards sustainable energy foster research in power system efficiency. This study innovates by merging the skill optimization

Received: December 28, 2023. Revised: January 19, 2024.

Table 1. Simulation results for different case studies

IEEE 30-bus System				IEEE 57-bus System			
Parameter	**Case 1**	**Case 2**	**Case 3**	**Parameter**	**Case 1**	**Case 2**	**Case 3**
P_{g1} (MW)	140.9845	176.1303	189.6791	P_{g1} (MW)	411.7158	245	245
P_{g2} (MW)	50	48.8527	52.1830	P_{g2} (MW)	0	0	10
P_{g5} (MW)	32.5	21.5228	22.5719	P_{g3} (MW)	30	59.9998	60
P_{g8} (MW)	22.5	22.2324	30.5171	P_{g6} (MW)	0	0	7.5
P_{g11} (MW)	20	12.2624	20.0001	P_{g8} (MW)	579.5	860.3416	857.7590
P_{g13} (MW)	26	12.0778	15.0007	P_{g9} (MW)	0	0	5
V_{g1} (p.u.)	1.0000	1.0500	1.0500	P_{g12} (MW)	259.5	139.8202	142.9950
V_{g2} (p.u.)	1.0250	1.0384	1.0389	V_{g1} (p.u.)	1.0000	1.0261	1.0296
V_{g5} (p.u.)	1.0000	1.0119	1.0126	V_{g2} (p.u.)	1.0000	1.0162	1.0196
V_{g8} (p.u.)	1.0000	1.0208	1.0213	V_{g3} (p.u.)	1.0000	1.0095	1.0096
V_{g11} (p.u.)	1.0000	1.0500	1.0500	V_{g5} (p.u.)	1.0000	1.0279	1.0284
V_{g13} (p.u.)	1.0250	1.0604	1.0642	V_{g8} (p.u.)	1.0000	1.0600	1.0600
P_{loss} (MW)	8.585	9.679	11.552	V_{g9} (p.u.)	1.0000	0.9962	0.9966
Q_{loss} (MVAr)	34.43	39.24	51.03	V_{g12} (p.u.)	1.0000	0.9965	0.9993
Cost ($/hr)	828.5192	803.13	935.2408	P_{loss} (MW)	29.916	54.362	54.954
				Q_{loss} (MVAr)	135.09	239.39	240.99
				Cost ($/hr)	35296.34	37589.34	37628.8

Table 2. Comparison in IEEE 30-bus system

Method	Cost ($/hr)	P_{loss} (MW)
Proposed	803.13	9.679
MATPOWER [1]	803.13	9.679
SMA [5]	802.5449	9.5232
MOPSO [8]	802.39	3.58
MOSGA [16]	800.6248	8.9987
WMFO [13]	800.603	9.066
EEO [17]	800.4145	8.99217
ISSA [9]	800.4752	9.1044
Rao-3 [7]	799.9918	9.0613
FAHSPSO-DE [6]	799.8066	-
EWOA [4]	799.210	8.643
GTOT [14]	799.0831	8.6263
MPA [10]	799.0725	8.6223
ESMA [15]	798.9709	8.5752
WO-BSA [12]	797.251	8.097

Table 3. Comparison in IEEE 57-bus system

Method	Cost ($/hr)	P_{loss} (MW)
MOPSO [8]	41,853.00	13.00
MOSGA [16]	41709.1504	15.8628
SMA [5]	41697.1189	15.5557
ISSA [9]	41675.0203	14.529
Rao-3 [7]	41,659.2621	14.7262
FAHSPSO-DE [6]	41637.18	-
WMFO [13]	39359.123	31.796
MATPOWER [1]	37589.34	54.362
Proposed	**37589.34**	**54.362**

algorithm (SOA) with open-access wind farm trading and EV fleet integration in power flow optimization (OPF). The ISOA-based OPF employs opposition-based learning (OBL) to diversify populations, targeting multi-objective goals. It minimizes generation costs, transmission losses, and fosters open-access trading. This facilitates surplus wind energy use, bolstering grid resilience. Simulations on IEEE 30-bus and 57-bus systems confirm its effectiveness: improved system performance, cost reduction, minimized losses, and increased renewable resource utilization. This advancement embraces sustainable advantages, enriching modern power grids. In the IEEE 30-bus, standard fuel costs were $803.13/hr, rising to $935.2408/hr with extra trading. Similarly, in the IEEE 57-bus, standard costs were $37589.34/hr, increasing slightly to $37628.8/hr with additional trading. These findings validate the method's proficiency in tackling intricate optimization challenges, consistent with established benchmarks.

Conflicts of interest

The authors declare no conflict of interest.

Author contributions

Conceptualization, methodology, software and original draft preparation are done by M. V. Ramesh and K. Swarnasri; supervision, review, and formal analysis are done by P. Muthukumar and Ponnam Venkata Kishore Babu.

References

[1] R. D. Zimmerman, C. E. M. Sánchez, and R. J. Thomas, "MATPOWER: Steady-state operations, planning, and analysis tools for

power systems research and education", *IEEE Transactions on Power Systems*, Vol. 26, No. 1, pp. 12-19, 2010.

[2] G. Papazoglou and P. Biskas, "Review and Comparison of Genetic Algorithm and Particle Swarm Optimization in the Optimal Power Flow Problem", *Energies*, Vol. 16, No. 3, p. 1152, 2023.

[3] J. M. H. Ortiz, W. C. D. Oliveira, and J. R. Mantovani, "Optimal power flow problem solution through a matheuristic approach", *IEEE Access*, Vol. 9, pp. 84576-84587, 2021.

[4] M. H. N. Shahraki, S. Taghian, S. Mirjalili, L. Abualigah, M. A. Elaziz, and D. Oliva, "Ewoa-opf: Effective whale optimization algorithm to solve optimal power flow problem", *Electronics*, Vol. 10, No. 23, p. 2975, 2021.

[5] S. Khunkitti, A. Siritaratiwat, and S. Premrudeepreechacharn, "Multi-objective optimal power flow problems based on slime mould algorithm", *Sustainability*, Vol. 13, No. 13, p. 7448, 2021.

[6] E. Naderi, M. P. Kasmaei, F. V. Cerna, and M. Lehtonen, "A novel hybrid self-adaptive heuristic algorithm to handle single-and multi-objective optimal power flow problems", *International Journal of Electrical Power & Energy Systems*, Vol. 125, p. 106492, 2021.

[7] S. Gupta, N. Kumar, L. Srivastava, H. Malik, A. A. Moghaddam, and F. P. G. Márquez, "A robust optimization approach for optimal power flow solutions using Rao algorithms", *Energies*, Vol. 14, No. 17, p. 5449, 2021.

[8] R. Kyomugisha, C. M. Muriithi, and M. Edimu, "Multiobjective optimal power flow for static voltage stability margin improvement", *Heliyon*, Vol. 7, No. 12, 2021.

[9] S. A. E. Sattar, S. Kamel, M. Ebeed, and F. Jurado, "An improved version of salp swarm algorithm for solving optimal power flow problem", *Soft Computing*, Vol. 25, pp. 4027-4052, 2021.

[10] M. Z. Islam, M. L. Othman, N. I. A. Wahab, V. Veerasamy, S. R. Opu, A. Inbamani, and V. Annamalai, "Marine predators algorithm for solving single-objective optimal power flow", *PLOS One*, Vol. 16, No. 8, p. e0256050, 2021.

[11] J. Montano, O. D. Garzón, A. A. Muñoz, L. F. G. Noreña, and O. D. Montoya, "Application of the arithmetic optimization algorithm to solve the optimal power flow problem in direct current networks", *Results in Engineering*, Vol. 16, p. 100654, 2022.

[12] J. L. Priya and S. T. J. Christa, "An effective hybridized GWO-BSA for resolving optimal power flow problem with the inclusion of unified power flow controller", *IETE Journal of Research*, Vol. 69, No. 7, pp. 4605-4617, 2023.

[13] M. H. N. Shahraki, A. Fatahi, H. Zamani, S. Mirjalili, and D. Oliva, "Hybridizing of whale and moth-flame optimization algorithms to solve diverse scales of optimal power flow problem", *Electronics*, Vol. 11, No. 5, p. 831, 2022.

[14] A. Shaheen, A. Ginidi, R. E. Sehiemy, A. Elsayed, E. Elattar, and H. T. Dorrah, "Developed Gorilla troops technique for optimal power flow problem in electrical power systems", *Mathematics*, Vol. 10, No. 10, p. 1636, 2022.

[15] M. Farhat, S. Kamel, A. M. Atallah, M. H. Hassan, and A. M. Agwa, "ESMA-OPF: Enhanced slime mould algorithm for solving optimal power flow problem", *Sustainability*, Vol. 14, No. 4, p. 2305, 2022.

[16] T. H. Huy, D. Kim, and D. N. Vo, "Multiobjective optimal power flow using multiobjective search group algorithm", *IEEE Access*, Vol. 10, pp. 77837-77856, 2022.

[17] E. H. Houssein, M. H. Hassan, M. A. Mahdy, and S. Kamel, "Development and application of equilibrium optimizer for optimal power flow calculation of power system", *Applied Intelligence*, Vol. 53, No. 6, pp. 7232-7253, 2023.

[18] R. A. Swief, N. M. Hassan, H. M. Hasanien, A. Y. Abdelaziz, and M. Z. Kamh, "Multi-regional optimal power flow using marine predators algorithm considering load and generation variability", *IEEE Access*, Vol. 9, pp. 74600-74613, 2021.

[19] M. H. Hassan, S. Kamel, A. Selim, T. Khurshaid, and J. L. D. García, "A modified Rao-2 algorithm for optimal power flow incorporating renewable energy sources", *Mathematics*, Vol. 9, No. 13, p. 1532, 2021.

[20] M. Farhat, S. Kamel, A. M. Atallah, and B. Khan, "Optimal power flow solution based on jellyfish search optimization considering uncertainty of renewable energy sources", *IEEE Access*, Vol. 9, pp. 100911-100933, 2021.

[21] M. Ahmad, N. Javaid, I. A. Niaz, A. Almogren, and A. Radwan, "A bio-inspired heuristic algorithm for solving optimal power flow problem in hybrid power system", *IEEE Access*, Vol. 9, pp. 159809-159826, 2021.

[22] E. Kaymaz, S. Duman, and U. Guvenc, "Optimal power flow solution with stochastic wind power using the Lévy coyote optimization algorithm", *Neural Computing and*

Applications, Vol. 33, pp. 6775-6804, 2021.

[23] M. H. Sulaiman and Z. Mustaffa, “Optimal power flow incorporating stochastic wind and solar generation by metaheuristic optimizers”, *Microsystem Technologies*, Vol. 27, No. 9, pp. 3263-3277, 2021.

[24] A. K. Khamees, A. Y. Abdelaziz, M. R. Eskaros, A. E. Shahat, and M. A. Attia, “Optimal power flow solution of wind-integrated power system using novel metaheuristic method”, *Energies*, Vol. 14, No. 19, p. 6117, 2021.

[25] M. A. Ali, S. Kamel, M. H. Hassan, E. M. Ahmed, and M. Alanazi, “Optimal power flow solution of power systems with renewable energy sources using white sharks algorithm”, *Sustainability*, Vol. 14, No. 10, p. 6049, 2022.

[26] V. A. Preethi, A. Shunmugalatha, and C. K. Babulal, “Evolutionary-based multi-objective optimal power flow considering real-time uncertainties in wind farms and load demand”, *Electrical Engineering*, pp. 1-21, 2023.

[27] W. N. Abed, “Solving Probabilistic Optimal Power Flow with Renewable Energy Sources in Distribution Networks Using Fire Hawk Optimizer”, *E-Prime-Advances in Electrical Engineering, Electronics and Energy*, Vol. 6, p. 100370, 2023.

[28] M. H. Hassan, S. Kamel, J. L. D. García, and R. J. Molu, “Integrating renewable energy and V2G uncertainty into optimal power flow: A gradient bald eagle search optimization algorithm with local escaping operator”, *IET Renewable Power Generation*, pp. 1-34, 2023.

[29] M. H. Hassan, S. Kamel, A. Alateeq, A. Alassaf, and I. Alsaleh, “Optimal Power Flow Analysis with Renewable Energy Resource Uncertainty: A Hybrid AEO-CGO Approach”, *IEEE Access*, Vol. 11, pp. 122926- 122961, 2023.

[30] T. H. Huy, H. T. Doan, D. N. Vo, K. H. Lee, and D. Kim, “Multi-objective optimal power flow of thermal-wind-solar power system using an adaptive geometry estimation based multi-objective differential evolution”, *Applied Soft Computing*, Vol. 149, p. 110977, 2023.

[31] M. M. Emam, E. H. Houssein, M. A. Tolba, M. M. Zaky, and M. H. Ali, “Application of modified artificial hummingbird algorithm in optimal power flow and generation capacity in power networks considering renewable energy sources”, *Scientific Reports*, Vol. 13, No. 1, p. 21446, 2023.

[32] T. M. Le, X. C. Le, N. N. Huynh, A. T. Doan, T. V. Dinh, and M. Q. Duong, “Optimal power flow solutions to power systems with wind energy using a highly effective meta-heuristic algorithm”, *International Journal of Renewable Energy Development*, Vol. 12, No. 3, pp. 467-477, 2023.

[33] F. Daqaq, M. H. Hassan, S. Kamel, and A. G. Hussien, “A leader supply-demand-based optimization for large scale optimal power flow problem considering renewable energy generations”, *Scientific Reports*, Vol. 13, No. 1, p. 14591, 2023.

[34] D. H. Wolpert, “The Implications of the No-Free-Lunch Theorems for Meta-induction”, *Journal for General Philosophy of Science*, Vol. 54, pp. 421-432, 2023.

[35] H. Givi and M. Hubalovska, “Skill Optimization Algorithm: A New Human-Based Metaheuristic Technique”, *Computers, Materials & Continua*, Vol. 74, No.1, pp. 179-202, 2023.